OFC

Technical Conference: 06 – 11 June 2021
Exhibition: 07 – 11 June 2021

A Virtual Conference - Pacific Daylight Time (UTC-07:00)

ABOUT | SCHEDULE | PROGRAM & SPEAKERS | EXHIBIT & INDUSTRY PROGRAMS | EXHIBIT AT OFC | REGISTRATION

HOME

About

- Committee
- The OFC Blog
- Photo Gallery
- Video Library
- Conference Archives
- 2020 Celebrating 50 Years of Light-speed Connections
- Event Policies & Terms
- Contact Us

CONFERENCE ARCHIVES

2020 – San Diego, California, USA

Program (PDF)
Conference Papers
Technical Sessions
Authors and Presiders

View Presentations

Previous Years

OFC | The Virtual Conference and Exhibition

Welcome | Submission

Contact Information

OSA Support	cstech@osa.org
Web	http://www.ofcconference.org

OFC 2021
6-10 June 2021
San Francisco, California, USA

CONTRIBUTED SUBMISSION DEADLINE: 26 January 2021, 12:00 noon EDT (16.00 GMT)

Need Assistance or Have Questions?
If you experience technical issues while trying to submit your work, please contact ScholarOne User Support by clicking the Help link at the top of the page.

If you have questions regarding the OSA Optical Fiber Communication Conference and Exposition, please visit http://help.osa.org.

Presentation Details | Paper

W6A.27
Entanglement Blocking in DLCZ-Based Networks
Presenter: Ian Tillman , *University of Arizona*
Presentation Details | Paper

W6A.28
107.6 Tb/s GMI Throughput Over 220 km SSMF Using Discrete C- and L-Band Amplification Across >12 THz
Presenter: Iosif Demirtzioglou , *Huawei Technologies France*
Presentation Details | Paper

W6A.29
Non-Volatile Operation of a Si PN Ring Resonator With a Ferroelectric Capacitor
Presenter: Seung-min Han , *Korea Institute of Science & Technology*
Presentation Details | Paper

W6A.30
Low-Complexity Symbol-Rate Rx DSP for Short-Reach Optical Coherent Transmission Systems
Presenter: Jianhong Ke , *Huawei Technologies Canada Research Center*
Presentation Details | Paper

W6A.31
Linewidth Limit of a Single Longitude-Mode Fiber Laser With Different Cavity Length
Presenter: Jianming Shang , *Beijing Univ of Posts & Telecom*
Presentation Details | Paper

W6A.32
EML-Based 200-Gbit/s/λ DMT Signal Transmission Over 10-km SSMF Using Entropy Loading and Simplified Volterra Equalization
Presenter: Jing Zhang , *Univ of Electronic Science & Tech China*

Non-Volatile Operation of a Si PN Ring Resonator with a Ferroelectric Capacitor

Seung-Min Han[1,2,3], Dae-Won Rho[2,3], Dae-Hwan Ahn[1], Jin-Dong Song[1], Woo-Young Choi[2*], Jae-Hoon Han[1]**
[1]*Center for Opto-Electronic Materials and Devices, Korea Institute of Science and Technology (KIST), Seoul, 02792, South Korea,*
[2]*Department of Electrical and Electronic Engineering, Yonsei University, Seoul, 03722,* [3]*contributed equally to this work.*
*wchoi@yonsei.ac.kr, **hanjh@kist.re.kr

Abstract: We demonstrated the non-volatile operation of a Si PN ring resonator with a ferroelectric $HfZrO_2$ capacitor. Due to the polarization in the $HfZrO_2$ capacitor, the resonance wavelength of the ring resonator shows the bi-stable operation.

1. Introduction

An optical phase shifter is a key component for optical modulators and switches. Among the various phase change schemes in silicon (Si) photonics platform, a free-carrier plasma dispersion effect in Si is commonly used for a CMOS-compatible, fast, and effective optical phase shifter. To change the free carrier concentration in Si, a PN junction with a ring resonator is widely used for the realization of high-speed and compact optical modulators and switches [1]. There are also many applications using this Si PN ring resonator, such as a large-scale switching array [2] and neuromorphic photonics [3]. To achieve efficient and multi-functional optical phase shifters for these applications, the non-volatile or bi-stable operation of the optical phase shifter is widely investigated using a phase-change material (PCM) [4] or a ferroelectric $BaTiO_3$ (BTO) [5]. However, these approaches have several problems, such as high loss due to the metal phase of PCM and non-CMOS-compatible materials or processes. In this paper, we demonstrate the feasibility of a non-volatile phase shifter using a Si PN ring resonator with a capacitor realized with the ferroelectric hafnium-zirconium oxide ($HfZrO_2$; HZO), a state-of-art ferroelectric material in the CMOS-compatible technology [6].

2. Si PN Ring Resonator with Ferroelectric HZO Capacitor

To achieve non-volatile operation of an optical phase shifter with PN junction, a ferroelectric capacitor is connected to Si PN ring resonator in series as shown in Fig. 1(a). Memory operation in the ferroelectric capacitor enables the bi-stable operation of the Si PN junction [7]. In this system, two states are expected. First, after the reverse bias is applied, the depletion layer of the PN junction is expanded compared to the initial state of the PN junction because of the remnant polarization (P_r) in the ferroelectric capacitor as shown in Fig. 1(b). After the forward bias is applied, the depletion layer becomes narrower compared to the initial state because of the opposite remnant polarization as shown in Fig. 1(c). The depletion layer difference between the two states makes the difference in the resonance wavelength for the Si ring resonator. As shown in Fig. 1(a), a voltage is applied to the series connection, the applied voltage is separated according to Eq. (1), where V_{Ferro}, V_{PN}, C_{Ferro}, and C_{PN} are the voltage and capacitance of the ferroelectric capacitor and the Si PN ring resonator, respectively. Therefore, capacitance matching between the ferroelectric capacitance and the PN junction capacitance is important in order to increase P_r, which decides the non-volatile window of this system. In this paper, we investigated the feasibility of the non-volatile operation using the series connection of a Si PN ring resonator and a ferroelectric capacitor. The resonance wavelength shift of the ring resonator was investigated after applying and removing the forward or reverse bias voltage. We also investigated the relationship between the resonance wavelength shift and the capacitance ratio of a ferroelectric capacitor and a PN resonator.

$$V_{Ferro} = V_{input} \times \frac{C_{PN}}{C_{Ferro} + C_{PN}} \quad (1)$$

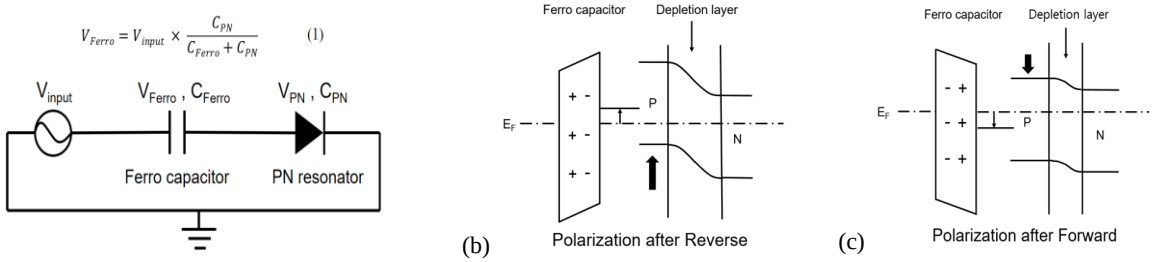

Fig. 1. Schematic of a ferroelectric capacitor and a Si PN ring resonator series connection. (a) circuit model, (b) energy band diagram after reverse bias and (c) energy band diagram after forward bias.

2.1 Characteristic of Ferroelectric HZO capacitor

We fabricated a metal-ferroelectric-metal (MFM) capacitor using HZO. The fabrication process flow, schematics, and SEM image of the crossbar HZO capacitor are shown in Fig. 2(a). First, a 60-nm-thick tungsten (W) layer for a bottom electrode was deposited on an Al_2O_3 substrate by DC sputtering. A 10-nm ferroelectric HZO layer was deposited by the atomic layer deposition (ALD) technique at 250˚C using TEMAHf, TEMAZr, and H_2O as Hf, Zr, and O precursors, respectively. A 60-nm-thick W top electrode was formed by the lift-off process. Ti/Au pads were also deposited on the bottom and top electrodes. Then, a ferroelectric capacitor was annealed at 500˚C by the rapid thermal annealing (RTA) process in the N_2 atmosphere for 30 s. As shown in Fig. 2(a), the crossbar shape of the ferroelectric capacitor was fabricated successfully. Figure 2(b) shows a capacitance–voltage (C–V) curve at 100 kHz for the ferroelectric capacitor having the area of 4×4 μm^2. Positive and negative coercive voltages are about 0.8 V and -0.75 V, respectively. Figure 2(c) shows polarization–voltage (P–V) curves of the ferroelectric capacitor for various programming voltages. P–V measurement was performed using a triangular voltage pulse at 2.5 kHz after wake-up cycling. As shown in Fig. 2(c), the polarization in the ferroelectric capacitor is changed by the applied voltage; thus, capacitance matching between the PN resonator and the ferroelectric capacitor is important to control the remnant polarization at the ferroelectric capacitor, which decides the non-volatile window of resonance wavelength.

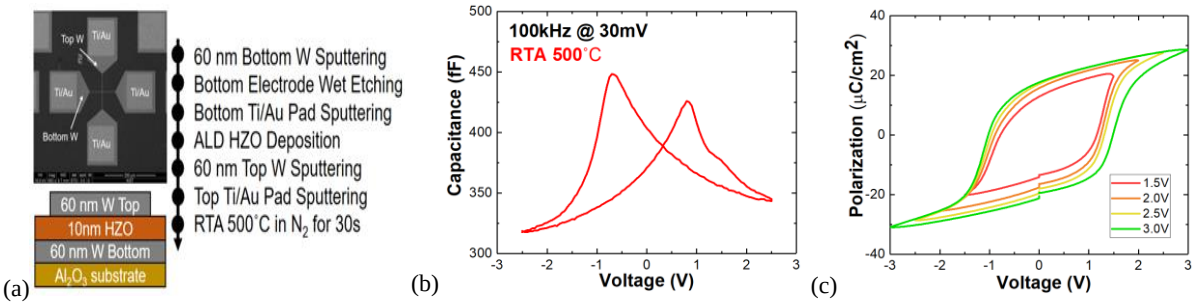

Fig. 2. (a) Fabrication process, cross-sectional schematic diagram and SEM image of ferroelectric capacitor, (b) C–V curve of ferroelectric capacitor, (c) P–V curve of ferroelectric capacitor.

2.2 Characteristics of Si PN Ring Resonator

Fig. 3(a) shows the transmission characteristics of the Si PN ring resonator used in this investigation. The device was fabricated by IHP's Si Photonics technology. It has 16-μm radius and 230-nm gap for ring and bus waveguides made up of 500-nm wide and 220-nm thick rib waveguides. In the lateral PN junction, the nominal peak carrier density is 7×10^{17}/cm^3 for the p-region and 3×10^{18}/cm^3 for the n-region. Figure 3(b) shows the C–V measured C–V characteristics for the Si PN ring resonator.

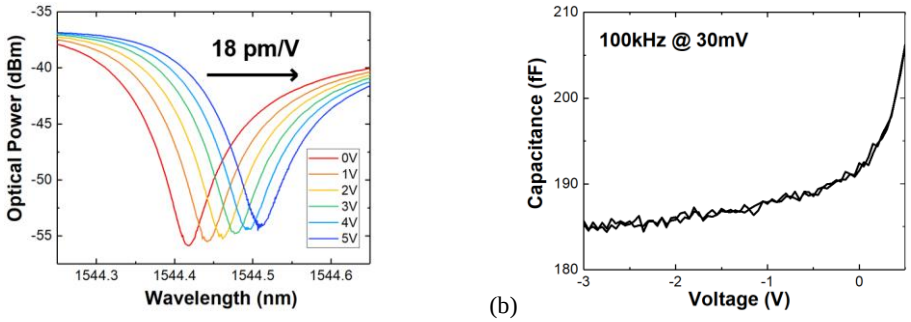

Fig. 3. (a) Modulation efficiency of Si PN Ring Resonator, (b) C–V Curve

3. Non-Volatile Phase Shift in Si PN Ring Resonator

The optical and electrical measurement setup used in the experiment is as shown in Fig. 4(a). The Si PN ring resonator was connected in series with the HZO capacitor with probes and an electrical cable. Before this connection, the triangular voltage purse of ±3 V was applied to the HZO capacitor for waking up the HZO capacitor [6]. After the HZO capacitor is connected to the Si PN ring resonator, the resonance wavelength is shifted left owing to the programmed HZO capacitor as mentioned before. Even if the forward bias of 2.5 V is

applied, the resonance wavelength does not change because it was already programmed before connection as shown in Fig. 3(b). The blue dashed-line in Fig. 4(c) shows the measured output power spectrum when the bias voltage of -6 V is applied. The wavelength shift of 79.2 pm is observed from red solid line to blue dashed line, which is same result to the wavelength shift when the reverse bias of -4.4 V is applied to the Si PN ring resonator. This voltage dividing at the Si PN ring resonator is caused by the ratio between the Si PN ring resonator and the HZO capacitor, which is approximately 2:5. Then, as shown in Fig. 4(c), when the bias voltage is changed from -6 V to 0 V, the measured output power spectrum shows the about 20 pm shift to the right compared to the curve obtained with the initial 0 V bias (from red solid line to yellow solid line). This is because the depletion width of the Si PN ring resonator is expanded by the polarization of the HZO capacitor as shown in Fig. 1(b). This resonance wavelength shift can be greatly enlarged by the large polarization in the HZO capacitor, which can be achieved by improvement in capacitance matching for the Si PN ring resonator and the HZO capacitor.

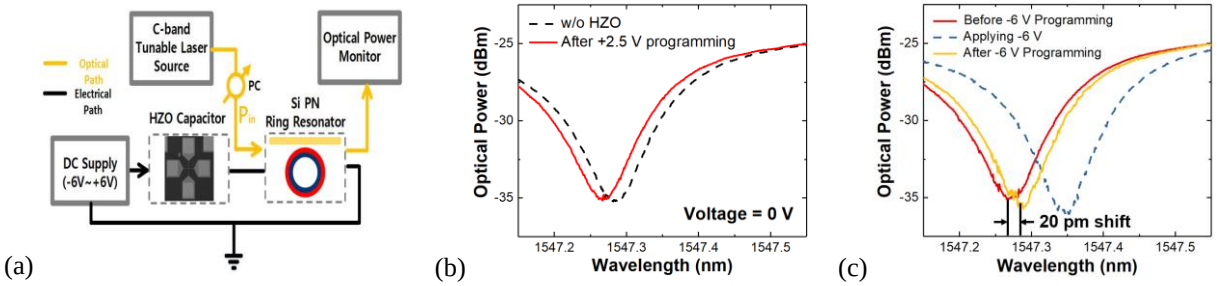

Fig. 4. (a) Circuit diagram of measurement setup, (b) optical power as a function of wavelength in forward mode, (c) reverse mode.

4. Conclusion

We successfully demonstrated the feasibility of a non-volatile optical phase shifter using the Si PN ring resonator with the ferroelectric HZO capacitor. Due to the remnant polarization in the HZO capacitor, we confirmed the bi-stable behavior between forward and reverse bias. We also confirmed the resonance wavelength of the Si PN ring resonator is shifted 20 pm between the two polarization states between forward and reverse bias. The wavelength shift can be enlarged by the polarization enhancement in the HZO capacitor. The presented non-volatile optical phase shifter can be a promising solution for high-efficient and multi-functional optical phase shifters.

5. Acknowledgements

This work was supported in part by the KIST Flagship Research Program under Grant 2E30100 and 2E31011, and in part by the National Research Foundation of Korea (NRF) Grant funded by the Korean Government Ministry of Science, ICT and Future Planning (MSIP) under Grant 2019M3F3A1A0207206912.

6. References

[1] Olivier Dubray *et al*., "Electro-Optical Ring Modulator: An Ultracompact Model for the Comparison and Optimization of p-n, p-i-n, and Capacitive Junction," *IEEE Journal of Selected Topics in Quantum Electronics* **22** (6), 3300110 (2016).

[2] A. W. Poon *et al*., "Cascaded Microresonator-Based Matrix Switch for Silicon On-Chip Optical Interconnection," Proc. *IEEE* **97** (7), 1216-1238 (2009).

[3] Elena Goi, Qiming Zhang, Xi Chen, Haitao Luan, and Min Gu, "Perspective on photonic memristive neuromorphic computing," *PhotoniX* **1** 1:3 (2020).

[4] Hanyu Zhang, Linjie Zhou, Jian Xu, Liangjun Lu, Jianping Chen, and B. M. A. Rahman, "All-optical non-volatile tuning of an AMZI-coupled ring resonator with GST phase-chang material," *Optics Letters* **43** (22), 5539-5542 (2018).

[5] Pascal Stark, Jacqueline Geler-Kremer, Felix Eltes, Daniele Caimi, Jean Fompeyrine, B. J. Offrein, Stefan Abel, "Novel Electro-optic Components for Integrated Photonic Neural Networks," *OFC*, M2I.4 (2020).

[6] Min Hyuk Park, Young Hwan Lee, Thomas Mikolajick, Uwe Schroeder, Cheol Seong Hwang, "Review and perspective on ferroelectric HfO_2-based thin films for memory applications," *MRS Communications* **8**, 795-808 (2018).

[7] Akira Inoue, "Memory effect on a Series Connection of a Ferroelectric Capacitor and a p-n Diode," *IEEE* **48** (7), 1438-1441 (2001).

Non-Volatile Operation of a Si PN Ring Resonator with a Ferroelectric Capacitor

Seung-Min Han[1,2,3] , Dae-Won Rho[2,3], Dae-Hwan Ahn[1], Jin-Dong Song[1], Woo-Young Choi[2*], Jae-Hoon Han[1**]

[1]Center for Opto-Electronic Materials and Devices, KIST

[2]Department of Electrical and Electronic Engineering, Yonsei University, [3]contributed equally to this work.

*wchoi@yonsei.ac.kr, **hanjh@kist.re.kr

Introduction

- Programmable Photonic Integrated Circuits (PICs) are widely investigated for many applications : LiDAR, optical communication, Biosensor, neuromorphic, etc.
- The optical phase shifter in PICs is a key component.

→ Programmable phase shifters make it possible to configure the functionality at run-time

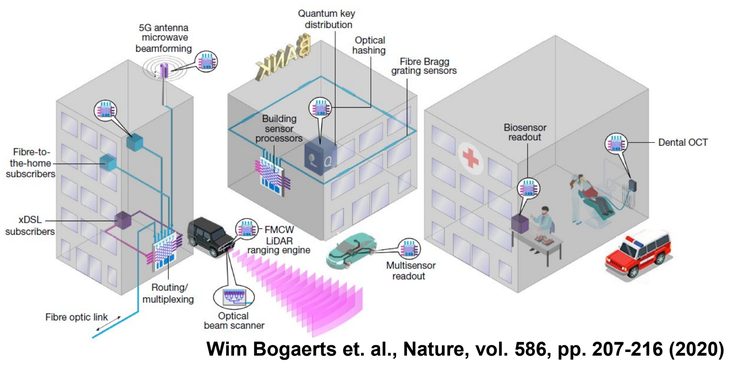

Wim Bogaerts et. al., Nature, vol. 586, pp. 207-216 (2020)

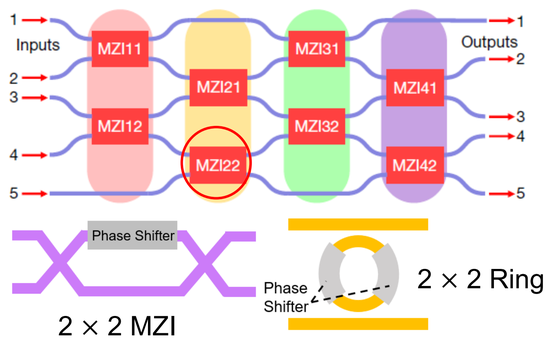

- To reduce the entire power consumption of programmable PICs,

→ Non-volatile operation of phase shifter is indispensable.

Objectives

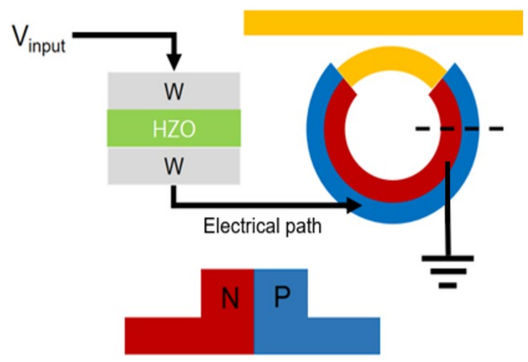

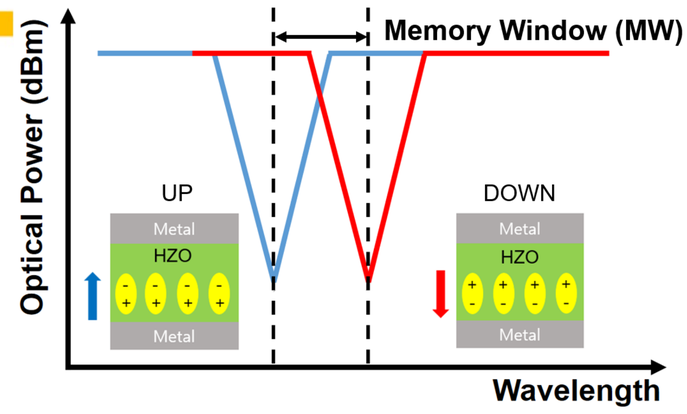

- A non-volatile phase shifter is implemented by the serial connection.

→ Si PN ring resonator + $HfZrO_2$ (HZO) ferroelectric capacitor

- We investigated non-volatile phase shifter using a Si PN ring resonator with a HZO ferroelectric capacitor.

→ CMOS-compatible technology

Non-Volatile Operation Using Remnant Polarization

Energy band diagram and transmission spectrum of FE cap & PN junction

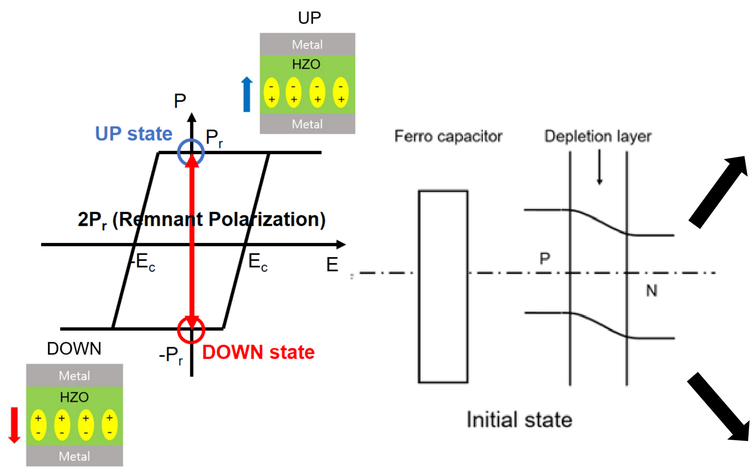

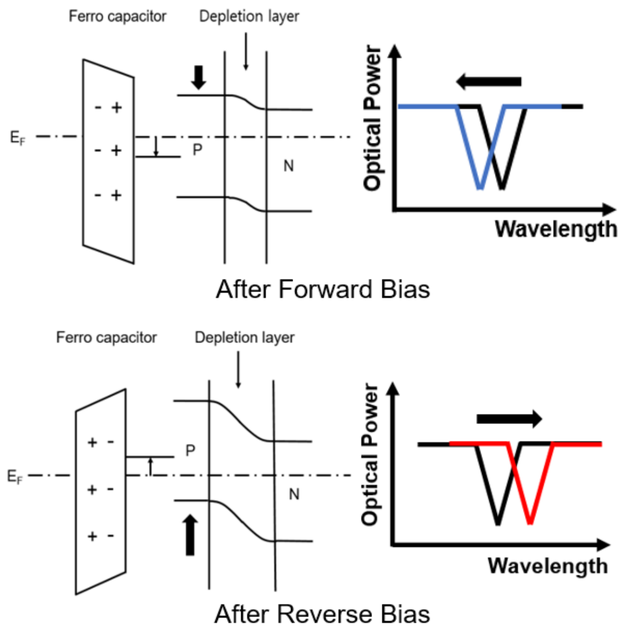

- Depletion width of the PN junction is fixed by the polarization of the HZO capacitor.
- Resonance wavelength shift is proportional to $2P_r$ of HZO capacitor.

$MW \propto 2P_r$

PN Ring Structure & Characteristics

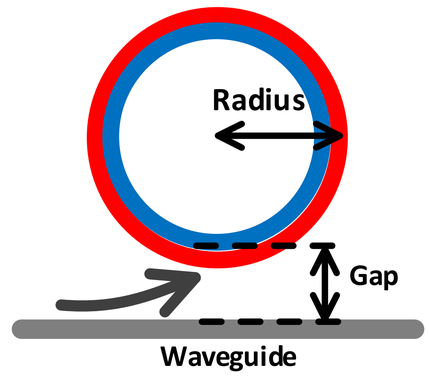

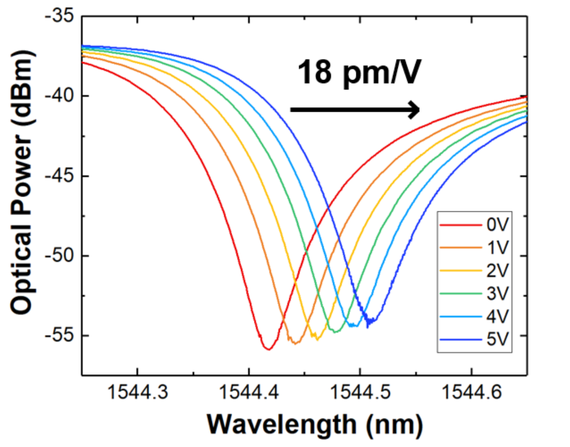

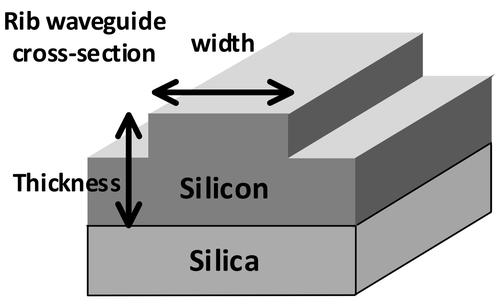

- **PN Resonator 230nm gap, 16μm radius**
- **Rib waveguide 220nm Thickness, 500nm width**
- **Efficiency 18pm/V**

HZO Capacitor Structure & Characteristics

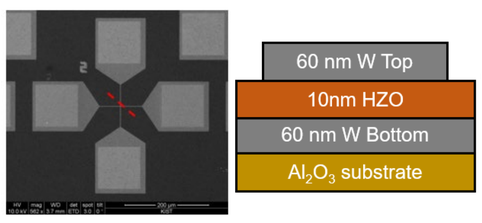

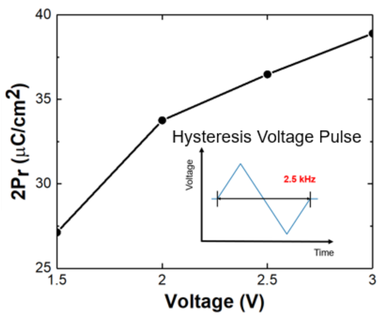

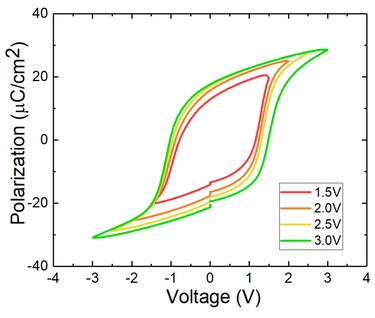

Capacitor Area : 4 × 4 (μm^2)

- 60 nm Bottom W Sputtering
- Bottom Electrode Wet Etching
- Bottom Ti/Au Pad Sputtering
- ALD HZO Deposition
- 60 nm Top W Sputtering
- Top Ti/Au Pad Sputtering
- RTA 500˚C in N_2 for 30s

- Crossbar-structured HZO capacitors were fabricated.
- The triangular voltage pulse of ± 3 V was applied to the HZO capacitor for polarization.
- Higher applied voltage can improve $2P_r$ of HZO capacitor.

Capacitance Matching Between PN & HZO

$$V_{Ferro} = V_{input} \times \frac{C_{PN}}{C_{Ferro} + C_{PN}}$$

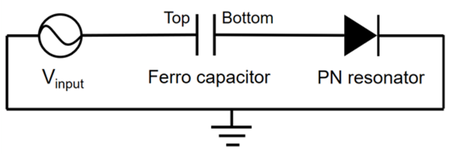

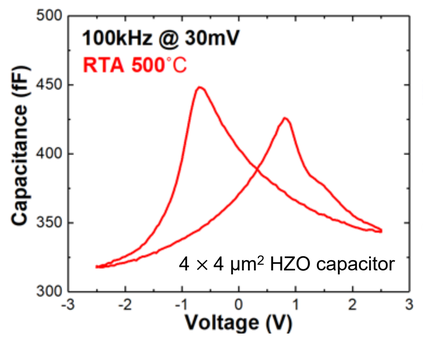

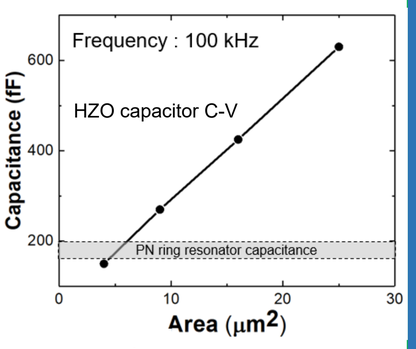

C_{Ferro} ↓ → V_{Ferro} ↑ → $2P_r$ ↑

- The Si PN ring resonator was connected in series with the HZO capacitor.

→ To achieve non-volatile operation of a Si PN Ring Resonator.

- To obtain higher $2P_r$ value, the divided voltage of the HZO capacitor should be larger.

Capacitance matching between FE capacitor & PN resonator is necessary.

Non-Volatile Resonator Operation with HZO

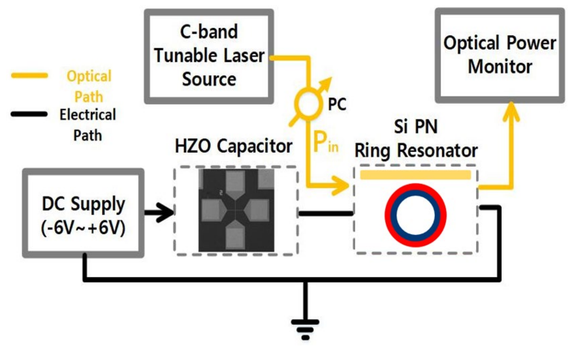

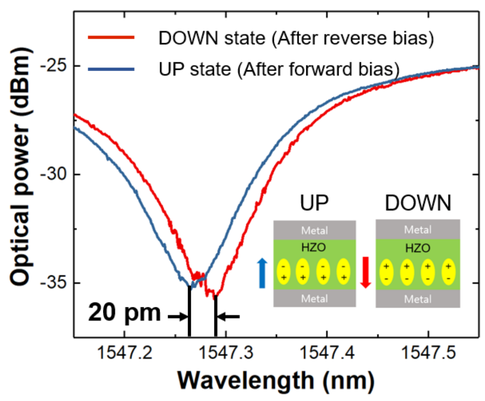

- The optical and electrical measurement setup for the experiment is shown above.
- Capacitance ratio → PN ring resonator : FE capacitor ≅ 2 : 5
- We confirmed the resonance wavelength of the Si PN ring resonator is shifted 20 pm between the two states.

Conclusion

- To achieve efficient & low power optical phase shifters for programmable PICs, non-volatile operation is needed.
- The feasibility of a non-volatile phase shifter was demonstrated using the CMOS-compatible Si PN ring resonator and HZO capacitor.
- To obtain higher memory window, capacitance matching between the HZO capacitor and the Si PN ring resonator is necessary.
- The non-volatile resonance wavelength shift of the Si PN ring resonator is 20 pm.
- The presented non-volatile optical phase shifter is a promising for high efficient and multi-functional optical phase shifters.

Acknowledgement :
This work was supported in part by the KIST Flagship Research Program under Grant 2E30100 and 2E31011, and in part by the National Research Foundation of Korea (NRF) Grant funded by the Korean Government Ministry of Science, ICT and Future Planning (MSIP) under Grant 2019M3F3A1A0207206912.

Korea Institute of Science and Technology

YONSEI UNIVERSITY 1885